Full Title: The Dynamics of IL-2 Deficiency: A Mathematical Exploration of Autoimmune Pathology

Running Title: Mathematical modeling of IL-2 dysregulation in autoimmunity

Authors: Jonathan M. Anzules*†, Kristen M. Valentine*†, Genevieve N. Mullins*†, Lihong Zhao§, Anh Diep*†, Katrina K. Hoyer†‡, Suzanne S. Sindi†§.

(use the following symbols in this order to designate authors' affiliations: *, †, ‡, §, ¶, ||, #, **, ††, ‡‡, §§, ¶¶, || ||, ##)

Affiliations:

*Quantitative and Systems Biology Graduate Program, University of California, Merced, CA 95340, USA; † Health Sciences Research Institute, University of California, Merced, CA 95340, USA; ‡ Department of Molecular and Cell Biology, University of California, Merced, CA 95340; USA, § Department of Applied Mathematics, University of California, Merced, CA 95340, USA

Table of Contents

Useful links

Links to tables, equations, individual figures, and link to figure descriptions

Abstract

Autoimmune diseases, driven by an immune system's inability to distinguish self- from foreign-antigens, present a complex interplay of factors whose pathogenesis is not fully understood. In response to this challenge, we developed a mathematical model to emulate the progression of systemic autoimmune disease that was fit to experimental data from spontaneous autoimmune reactions in the IL-2 deficient BALB/c mouse model (IL-2 knockout, KO). Our model simulates the dynamic interactions of IL-2 cytokine with CD4 T cells originating from both the thymus and spleen, which are crucial for maintaining immune tolerance and preventing autoimmune disease dysregulation. Our model-based comparative analysis identified deficient expansion trajectories in naive and regulatory T cells within the autoimmune state compared to the wild-type counterpart. A sensitivity analysis, using Latin Hypercube Sampling, elucidates early Treg dysfunction, critical parameters necessary for preventing autoimmune disease and dissects the systemic implications of IL-2 deficiency. This is the first published mathematical model that explores early autoimmune pathogenesis in IL-2 knockout mice, introducing a new way to study autoimmune development.

Introduction

Autoimmune diseases, including systemic lupus erythematosus (SLE), irritable bowel syndrome, and rheumatoid arthritis, impact approximately one in ten individuals (1, 2), leading to high healthcare costs and decreased quality of life for affected individuals (3, 4). Despite the recognition of specific risk factors (5–8) and a range of available treatment options (9–12), these disorders persist without a cure, and their prevalence is on the rise (13, 14). This escalating trend underscores the pressing need to unravel the developmental mechanics of autoimmune diseases. However, a clear understanding of autoimmune diseases' initiation and progression remains elusive (15). In this study, we introduce a mathematical model that depicts the development of a standard or autoimmune system—providing a sophisticated toolkit to explore the dynamics of autoimmune pathogenesis.

Interleukin-2 (IL-2) cytokine production is notably decreased in SLE patients, affecting various aspects of host immunity, including CD4 T cell development and function (16). IL-2 governs the functionality and survival of CD4 regulatory T cells (Tregs), indispensable in preventing autoimmune diseases (16). The IL-2 deficient mouse model (IL-2 knockout, KO) has a weakened Treg population, resulting in the spontaneous onset of systemic autoimmune disease (17). In this study, we take advantage of the known effects of IL-2 deficiency to cause autoimmune disease and replicate it in our simulation. The utility of the IL-2 KO mouse model is underscored by its ability to clearly indicate an autoimmune state through the marked increase in activation of autoreactive T cells (17–19). These cells can be characterized by activation markers, including CD69, CD44, and CD62L, especially when compared to the wild-type (WT) counterpart (23, 24)—a phenomenon paralleling other systemic autoimmune diseases (18,

20–26). Our mathematical model, calibrated with comprehensive cellular data from both WT and autoimmune IL-2 KO mice, allows us to simulate and scrutinize the systemic effects of IL-2 deficiency. Employing the least squares optimization method (27), we identify model parameters to capture the dynamics observed in these mouse models, from birth to the final stages of autoimmune disease development.

Comparative analysis between WT and IL-2 KO simulation results identified deficient expansion trajectories in the naive T cell and Treg population in an autoimmune setting relative to the WT. We interpreted these differences as symptoms of autoimmunity in our model. We employ Latin Hypercube Sampling (LHS) to study the consistency of these patterns. Our analysis offers a distinct perspective to the limited expansion potential of early peripheral Tregs, and identifies critical parameter values necessary to prevent the high levels of naive T cell activation seen in the IL-2 KO mice.

Materials and Method

Mice

BALB/c IL-2-KO mice were bred in our animal facility. BALB/c WT and IL-2 heterozygous littermates were used interchangeably as controls in all experiments, as no heterozygous difference from WT was observed. Male and female mice were used in all experiments. All mice were bred and maintained in our specific pathogen-free facility in accordance with the guidelines of the Department of Animal Research Services at UC Merced. The UC Merced Institutional Animal Care and Use Committee approved all animal procedures.

Organ Processing

Spleen and thymus were harvested, weighed, and mechanically dissociated into single-cell suspensions on days 0, 4, 7, 9, 12, 14, 15, and 18-20, with days 18-20 grouped as 'day 18+' to represent late-stage autoimmune disease, as mortality in IL-2 KO mice typically begins by day 18.1x ammonium chloride red blood cell lysis buffer was added to the sample, incubated for 30 seconds, and then diluted with phosphate-buffered saline (PBS; Omega) containing 2% fetal bovine serum (FBS; Omega).

Antibody Staining

The following antibodies were used in this study: TCR-β (FITC; eBioscience; H57-597), CD4 (PerCP-Cy5.5; eBioscience; RM4-5), CD8 (APC; Biolegend; 53-6.7), CD19 (PE-eFluor 610; eBioscience; 1D3), Foxp3 (PE; eBioscience; FJK-16s), Ki-67(PE Cy7; eBioscience; SolA15),

fixable viability dye (eFluor506; eBioscience), CD69 (APC-eFluor 780; H1.2F3), CD62L (PE; Biolegend; MEL-14), and CD44(FITC; Biolegend; IM7).

Spleen and thymus lymphocytes were surface stained in PBS plus 1% FBS with fluorochrome-conjugated antibodies recognizing CD4, CD8, CD19, TCR-β, CD44, CD62L, CD69 for 30 minutes at 4°C in the dark. Cells were washed with PBS/1%FBS, centrifuged at 4°C 400g for 5 mins, the supernatant discarded, and cells were fixed with Foxp3/Transcription Factor Fixation/Permeabilization Kit (eBioscience) according to the manufacturer's instructions for intracellular proteins Ki67 and Foxp3. Flow cytometry was performed on BD LSRII and data was analyzed using FCS Express version 4 (Denovo Software). Populations of interest assessed: Tregs ($CD4^+$,$CD8^-$, TCR-β^+, $Foxp3^+$), naive T cells ($CD4^+$, $CD8^-$, TCR-β^+, $CD44^-$,$CD62L^+$), and activated T Cells ($CD4^+$, $CD8^-$, TCR-β^+, $CD44^+$,$CD62L^-$). Replicating cells were identified based on Ki-67 expression, early activation by CD69+, and activated T cells by CD44+ and CD62L–. Total numbers were calculated using hemocytometer cell counts and flow cytometry data.

Parameter Estimation

A least squares minimization algorithm was used to find parameters that minimize the discrepancy between the model output and experimental data. This approach involves estimating 16 parameters (Table I) within specified ranges that reflect the data, while fixing 5 parameters obtained from literature and data (Table II). Our algorithm iteratively applies both ode15s, used to solve our mathematical model, a system of ordinary differential equations (ODEs), see Equations 1 - 4, and fmincon (28, 29), and a constrained nonlinear optimization algorithm that estimates parameter values until convergence to a local minimum. The error was quantified using an objective function that evaluates the difference between the simulation output (S) and experimental data (D) for each genotype (G = {WT, and IL-2 KO}), cellular population (B = {thymic derived naive T cells, thymic derived Tregs, naive derived activated T cells, self-replicating Tregs, self-replicating naive T cells, and self-replicating activated T cells}), and time point (J = {4, 7, 9, 12, 14, and 18+})

$$\text{Error} = \sum_{g=1}^{G} \sum_{b=1}^{B} \sum_{j=1}^{J} \left(\frac{S_{gbj} - D_{gbj}}{S_{gbj}} \right)^2.$$

We set the initial population sizes by calculating the means of each subpopulation from our study's day 0 mice. To determine an optimal parameter set, we calculated the mean error value from our optimization algorithm's distribution of error values (Median error value: 3309, Table SI). These optimal parameter values were then used as the initial conditions for our Latin Hypercube sampling experiments.

Latin Hypercube Sampling

We utilized Latin Hypercube Sampling (LHS) to explore the dominant behavioral patterns of our mathematical model. After choosing an optimal set of parameters, we independently varied key parameters around their initial conditions, allowing us to investigate the impact of parameter variations on the model's behavior. We used lhsdesign (30) to generate an LHS matrix of size *r*-by-*u*, where *r* is the number of simulation runs, and *u* is the number of parameters to be tested. The randomized parameter values were obtained from the inverse cumulative distribution function (CDF) of a continuous uniform distribution. For all LHS studies, we ran 3000 simulations with a +/- 60% variation of four parameters around their initial conditions. When visualizing results from LHS, we depict the mean, 10^{th}, and 90^{th} percentile.

Statistical Analysis

Data analysis was conducted using R (version 4.3.2). Normality of datasets was assessed with the Shapiro-Wilk test, followed by a combination of one-tailed t-tests and Mann-Whitney U tests (Fig. 1; Table SII). Analyses were conducted on datasets that included at least three samples ($n \geq 3$) per genotype for each day. Significance is indicated as $*p < 0.05$, $**p < 0.01$, and $p > 0.05$ is NS.

Results

Phenotypic Differences Between WT and IL-2 KO mice

IL-2-deficient (IL-2 KO) mice are a well-studied model of systemic autoimmune disease, known to spontaneously develop multiple clinically relevant autoimmune conditions (17–19). In BALB/c mice, IL-2 deficiency precipitates severe autoimmunity, leading to death by three weeks of age, yet the initiation and progression of autoimmunity in these mice are not clearly defined. To build a mathematical model that accurately depicts T cell development in both standard and autoimmune development, we collected T cell phenotypic data from WT and IL-2 KO mice from multiple time points during the first three weeks after birth.

Our analysis of spleen data reveals that during the initial stages of homeostatic expansion (4-12 days), activation markers of CD4 T cells do not exhibit significant differences between WT and IL-2 KO mice, except day 7 (Fig. 1A and 1B). On this day, IL-2 KO mice exhibited a significant increase in early activated CD4 T cells (CD4+CD69+) count (p-value: 1.47E-02; Table SII). From day 12 onwards, IL-2 KO mice consistently showed elevated activation levels, evidenced by an increase in early activated CD4 T cells (Fig. 1A and 1B) and fully activated CD4 T cells (CD4+CD44+CD62L–; Table SII). This ongoing increase in activation persisted into the later stages of autoimmune disease development, with significantly higher counts of non-proliferating activated T cells noted on days 12 and 18 (CD4+CD44+CD62L–KI-67–; Fig. 1D). Increase in the proliferation of activated T cell percentages was significant only on day 14 (CD4+CD44+CD62L–KI-67+; Fig. 1F), suggesting a systemic activation disorder in IL-2 KO mice.

While early activation data showed minimal differences, Treg (CD4+Foxp3+) percentages and total cell counts were significantly reduced in IL-2 KO mice on days 4, 7, and 9. In subsequent stages, Treg percentages continued to be significantly lower on days 14 and 18, though total Treg numbers did not significantly differ between genotypes in later stages (Fig. 1G and H).

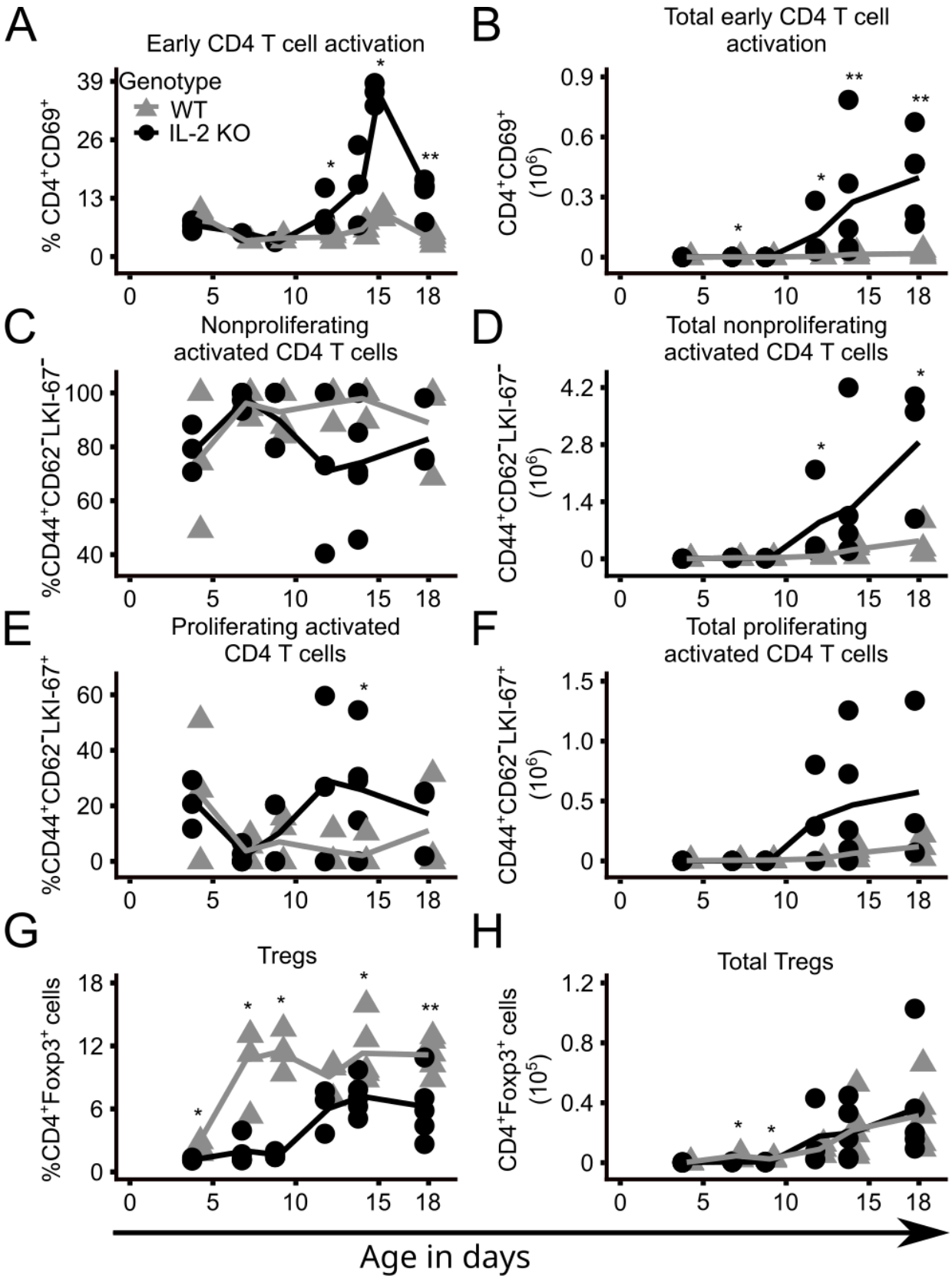
A
Early CD4 T cell activation
Genotype
WT
IL-2 KO
% CD4+CD69+
B
Total early CD4 T cell activation
CD4+CD69+ (10^6)
C
Nonproliferating activated CD4 T cells
%CD44+CD62-LKI-67-
D
Total nonproliferating activated CD4 T cells
CD44+CD62-LKI-67- (10^6)
E
Proliferating activated CD4 T cells
%CD44+CD62-LKI-67+
F
Total proliferating activated CD4 T cells
CD44+CD62-LKI-67+ (10^6)
G
Tregs
%CD4+Foxp3+ cells
H
Total Tregs
CD4+Foxp3+ cells (10^5)
Age in days

Figure 1 – Phenotypic differences in CD4 T cell activation and Treg populations between IL-2 KO and WT mice. Data from spleen results emphasize the characteristics of CD4 T cells and their subpopulations, highlighting the phenotypic variations observed between IL-2 KO mice (black circles) and WT mice (grey triangles), with each dot representing one animal (n =1-5, per day, per genotype). The figure displays the differences in (A) percentage and (B) total cell numbers of early activated T cells (CD4+ CD69+), (C) percentage and (D) total cell numbers of non-proliferating activated T cells (CD4+ CD44+ CD62L– Ki-67–), (E) percentage and (F) total cell numbers of proliferating activated T cells (CD4+ CD44+ CD62L– Ki-67+), and (G) percentage and (H) total cell numbers of regulatory T cells (CD4+ Foxp3+). Significance is indicated as *p < 0.05, **p < 0.01, and p > 0.05 is NS.

Model Development

Building upon the mathematical model by Khailaie et al. (31), our model depicts the interplay between the IL-2 cytokine (and lack thereof on), Treg survival, and functionality. Khailaie et al.'s model highlighted how discrimination between self- and non-self-antigens is determined by the immune system's dynamic structure and the cells' flow rate between compartments. While their insights formed a valuable foundation for our work, our model includes additional factors described below (Fig. 2; Equations 1-4).

$$\frac{dN}{dt} = \mu N\left(1 - \frac{N}{K_N}\right) + s_n N - \beta N / \left(1 + \left(R\left(\frac{I}{H_I + I}\right) / H_\beta\right)\right) - \gamma_N N \quad (1)$$

$$\frac{dT}{dt} = \beta N/\left(1 + \left(R\left(\frac{I}{H_I+I}\right)/H_\beta\right)\right) + s_T T - \theta RT\left(\frac{I}{H_\theta+I}\right) - \gamma_T T \quad (2)$$

$$\frac{dR}{dt} = \alpha R\left(1 - \frac{R}{K_R}\right) + s_R R + cN - \gamma_R R/\left(1 + I/H_{\gamma R}\right) \quad (3)$$

$$\frac{dI}{dt} = pT - e_T IT - e_R IR - \lambda I. \quad (4)$$

This model tracks the development of an immune system from a population of cells emerging from the thymus (either naive T cells or Tregs). The previous study considers a constant rate of production. During our model's evolution, we discerned that the constant Treg and naive T cell production rate, as proposed by Khailaie et al., did not align with our experimental data. Their framework, rooted in a steady-state perspective, failed to encapsulate the nuanced dynamics of a growing and developing immune system. Instead of the linear growth pattern, our data revealed distinct lag and exponential phases (Fig. 1 & 3), characteristic of biological growth patterns, especially in cellular populations. Our solution was to deploy a logistical growth equation instead of Khailaie et al.'s constant production rate. This amendment was crucial: the revised rate equations captured the lag and exponential phases and echoed them across all our cellular populations. This modification elucidated the representation of thymus-derived naive T cells (N) and Treg (R) populations represented by $\mu N\left(1 - N/K_N\right)$ and $\mu N\left(1 - N/K_N\right)$ respectively.

Upon recognition of an antigen, whether self-derived or foreign, naive T cells may initiate differentiation into Tregs (c) and activated T cells (β). Beyond differentiation, all three cellular populations—naive T cells, activated T cells, and Tregs— undergo self-replication (s_N, s_T, s_R).

All populations also have designated rates for natural turnover and half-lives, represented by γ_N, γ_T, γ_R and λ, respectively.

The survival, expansion, and functionality of Tregs are intrinsically linked to IL-2 availability (I) (18, 32). IL-2 is primarily produced by activated T cells (p) (32–34), and its consistent consumption occurs in both Tregs (e_R) and activated T cells (e_T). A key distinction between our model and the Khailaie et al. model lies in our treatment of IL-2's influence on Treg dynamics. Unlike the prior model, ours incorporates dual functions of IL-2: enhancing Treg survivability and their suppressive capacities. To depict this relationship, our model employs a Hill suppressive function $((1 + I/H_{\gamma R})^{-1}$, which increases the probability of Treg survival by decreasing the Treg death rate (γ_R). An increase in IL-2 availability leads to a corresponding decrease in the Treg death rate, with $H_{\gamma R}$ denoting the half-maximal IL-2 point for Treg survival. To measure the impact of IL-2 on Treg survival under varying cytokine concentrations, we introduce the Treg Survival Factor (TSF). The TSF is mathematically formulated as:

$$1 - (1 + I/H_{\gamma R})^{-1} \qquad (5),$$

ranging from 0 to 1, where higher values signify greater survival probabilities due to effective IL-2 signaling (Fig. 4B).

Tregs play a critical role in regulating activated T cell populations via multiple methods. Tregs can modulate the function and maturation of dendritic cells (DC) (35–41), a type of

antigen-presenting cell that presents antigenic material to T cells during T cell activation. Within this framework, we represent naive T cell activation by DCs as a constant rate β and Treg-mediated suppression of naive T cell activation as the term:

$$\left(1 + \left(R\left(\frac{I}{H_I + I}\right)/H_\beta\right)\right),$$

where H_β and H_I set the threshold for the regulatory influence on naive T cell activation by Tregs and IL-2, respectively. In our model, 'clearance' encompasses the Treg-mediated cytotoxicity of activated T cells (42–46) and the induction of anergy, rendering the T cells functionally inactive (47). This process is mathematically represented by the term:

$$\theta RT\left(\frac{I}{H_\theta + I}\right),$$

where θ is the rate constant for clearance and H_θ sets the half promotion rate by IL-2.

With the structure of our mathematical model set, we simulate the dynamics of both a WT and IL-2 KO system. The IL-2 KO mouse model cannot properly produce IL-2 cytokine; however, microchimeric maternal cells can produce IL-2 (48) and Tregs can compensate for the lack of IL-2 by consuming other cytokines such as IL-7, IL-10, and IL-15 (49–51) to maintain their survival and functionality. To represent this compensatory mechanism in our model, we reduce the production of IL-2 (p) to 10% of the WT value in the IL-2 KO simulation (p_{KO}) while keeping all other parameters identical to the WT simulation (Table II). This difference allows us to isolate the specific effects of IL-2 deficiency on the immune system while accounting for the compensatory mechanisms that may be at play *in vivo*.

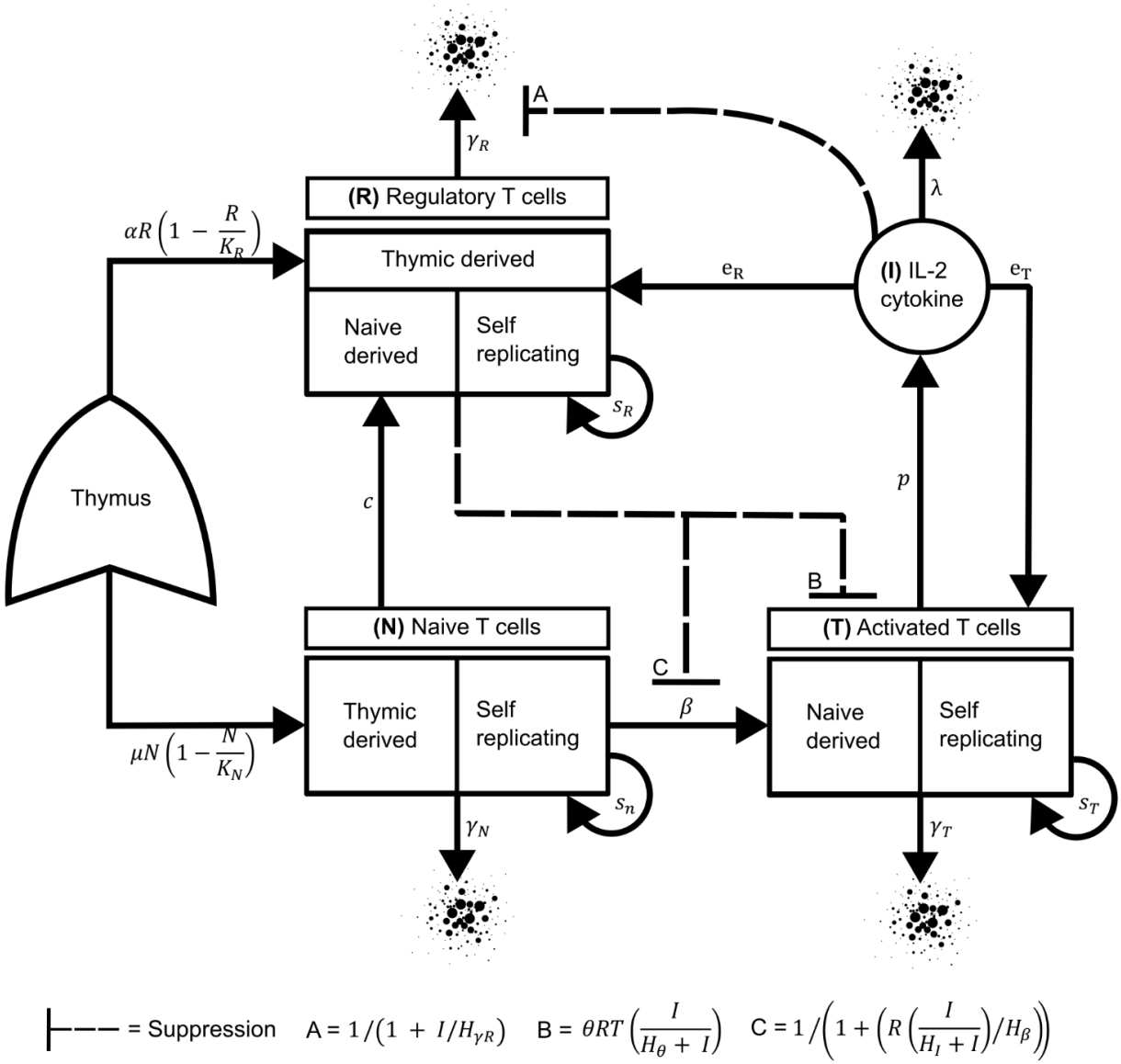

Figure 2 – Modeling T cell and Treg interactions during homeostatic expansion. This visual representation illustrates our system of ordinary differential equations (equations 1-4). The solid lines with arrows depict the flow of cellular and cytokine populations, while dashed lines with a bar head indicate suppression. The model starts with the supply of naive T cells and Tregs through their production in the thymus. Naive T cells can differentiate into Tregs at a rate denoted by *c*and become activated T cells at a rate denoted by β. Each cell population—naive T cells, activated T cells, and Tregs—has its self-replication rate (s_N, s_T, s_R) and death rate (

γ_N, γ_T, γ_R). Activated T cells produce IL-2 cytokine at the rate p that Tregs consume at the rate $e_R$and by activated T cells at the rate e_T. The terms A, B, and C represent the influence of IL-2, inhibiting the death rate of Tregs (A), increasing the clearance rate of activated T cells (B), and increasing the suppression rate on naive T cell activation (C). The only difference between the WT and IL-2 KO simulations is the production rate of IL-2 (p). In the WT model p is set at 1000 molecules per cell per hour, while the IL-2 KO model is set at 100 molecules per cell per hour (p_{KO}).

Simulation-Based Analysis of Autoimmune Dysregulation

During the early stages of homeostatic expansion (days 0 - 9), the cellular expansion trajectories of both the WT and IL-2-KO mice are all in the lag phase (Fig. 1 & 3). Post day 9, all cellular populations transition to exponential growth. On day 12, marked differences in immune activation between genotypes are seen in our data and simulation (Fig 1A-B, Fig 3A; Table SII). After our parameter estimation procedure, we were able to replicate these primary growth patterns of the cellular populations (Fig. 3).

The increase in activation signatures in the IL-2 KO data relative to the WT was one of the main defining features we wished to capture with our model as a prerequisite for further analysis (Fig 1A-B; Fig 3A). Our optimized parameter set successfully captures the qualitative difference between WT and autoimmune activation (IL-2 KO) (Fig. 3A; Simulation comparison), establishes a basis for inference analysis, and enables a detailed comparison of expansion trajectories across identical cellular populations of both genotypes.

In analyzing the total naive T cell populations (Fig. 3B), the IL-2 KO simulation demonstrated a reduced expansion trajectory relative to the WT, serving as a symptomatic marker of the autoimmune condition in our simulations. By the end of the simulation, the IL-2 KO genotype is markedly lower than its WT counterpart, with a difference of more than 250k cells (Fig. 3B, Simulation comparison), indicating widespread activation of CD4 T cells. This surge in naive T cell activation and declining numbers likely reduces the pool of naive T cells available for Treg differentiation (Fig. 3C's fourth column).

Supported by our analysis and corroborated by external experimental evidence, the homeostatic expansion of Tregs predominantly hinges on Treg proliferation and their differentiation from naive T cells (52, 53). Our data and simulation demonstrate this dynamic in Fig. 3C, where thymic-derived Tregs (column 3) contribute far less to the total Treg numbers (column 1) compared to Treg proliferation (column 2) and naive-derived Tregs (column 4). Our simulation reveals another symptom of the autoimmune state: a reduction in the total Treg count in the IL-2 KO simulation (SFig. 1A).

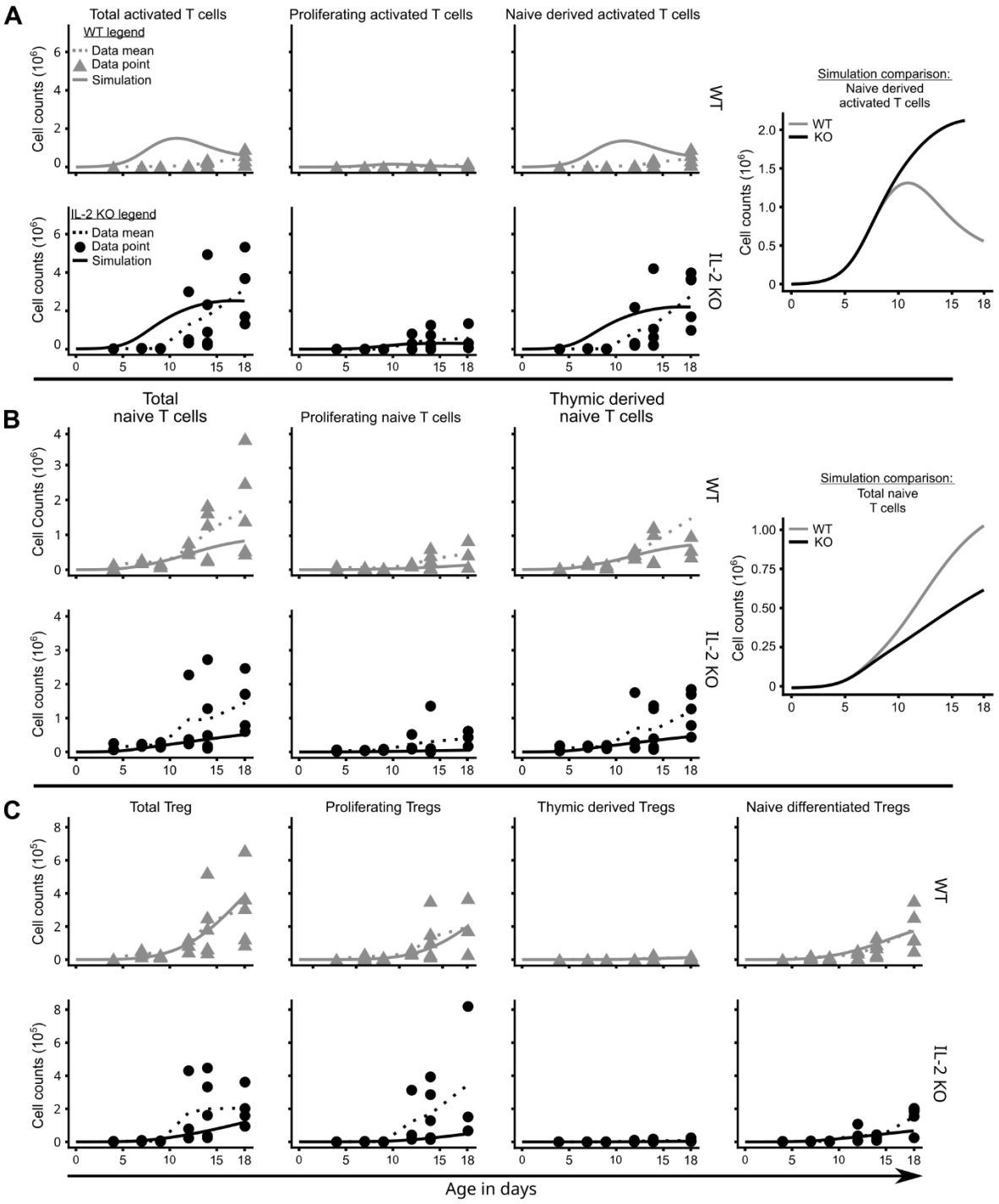

Figure 3 – Comparative dynamics of homeostatic expansion and autoimmune dysregulation in IL-2 KO and WT models. The figure includes data collection results (black circles and grey triangles), the mean of the data (shown as a dotted line), and simulation results

(depicted by solid lines). (A-B) Each section consists of a table of figures comparing IL-2 KO (top row) and WT (bottom row) data with corresponding simulation results. In the simulation comparisons, the WT is represented by a grey line, and a black line represents the IL-2 KO. (A) Activated T cell population and its sub-populations are shown. From left to right, each column represents the data for total activated T cells, proliferating activated T cells, and naive derived activated T cells. (B) The naive T cell population and its sub-populations are presented. From left to right, each column represents the data for total naive T cells, proliferating naive T cells, and thymic derived naive T cells. (C) Tregs and their sub-populations are displayed. From left to right, each column represents the data for total Treg, proliferating Tregs, thymic derived Tregs, and naive derived Tregs.

Dysfunction Created by IL-2 Deficiency

Our analysis of Treg population dynamics within the IL-2 KO simulations revealed a reduction in Treg numbers over time (SFig. 1A), indicating a disruption in homeostatic mechanisms due to IL-2 deficiency. Investigating these dynamics further could reveal insights into the Treg frequency decline observed in IL-2 KO mice (Fig. 1G). IL-2 is a survival signal of Tregs; activation of the IL-2 receptor complex initiates the STAT5 pathway-mediated signal transduction (54) to promote the expression of anti-apoptotic and survival genes, such as Bcl-2 (55). Further scrutiny of Treg dynamics in our simulation shows an increase in the number of Tregs dying in the IL-2 KO from the beginning (SFig. 1B). In addition, other research has shown that artificially increasing the survival of Tregs in a system with compromised IL-2/IL-2 receptor dynamics can expand the Treg population size (56, 57). However, this does not save the system from developing autoimmune diseases (58). In our simulations, without directly influencing the

Treg proliferation by IL-2 cytokine, we still see in our model that the proliferative rate of Tregs is diminished in the IL-2 KO simulation (SFig 1C).

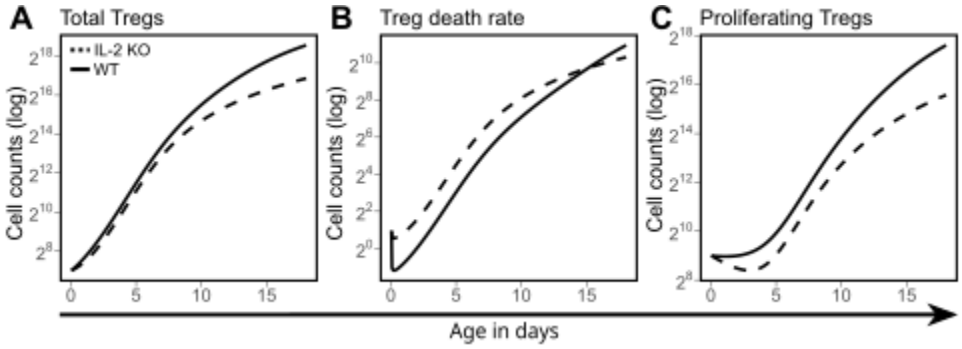

Supplementary Figure 1 – Comparison of Treg population dynamics in wild-type and knock-out simulations: Plots display the log transformation of various Treg population rates and sizes. The solid lines indicate WT simulations, while the dashed lines reflect IL-2 KO simulations. (A) Total Treg population size (B) Treg death rate and (C) Treg proliferation rate

We utilized the LHS method to investigate the stability of these deregulatory processes in IL-2 KO Treg populations. By varying four key parameters affecting Treg survival: Treg death rate (γ_R), half-maximal IL-2 point for Treg survival ($H_{\gamma R}$), and IL-2 production rate for WT and IL-2 KO cells (p and p_{KO}), we assessed the consistency of dysregulation seen in the IL-2 KO Treg population (Fig. 4). Our analysis revealed a decrease in the availability of IL-2 in the IL-2 KO simulation (Fig. 4A), leading to a lower value of the Treg Survival Factor (Equation: 5; Fig. 4B).

Despite the randomization, the early increase in Treg death rate in the IL-2 KO population persisted (Fig. 4C, bottom panel). Notably, the LHS analysis also showed that while the death rate of Tregs in the WT population eventually surpassed that of the IL-2 KO population over time (Fig. 4C, top panel), the IL-2 KO Tregs exhibited a slightly elevated death rate during the most vulnerable stages of development (Fig. 4C, bottom panel).

The difference in apoptotic Tregs between the genotypes is important, as it can affect the expansion potential by removing available Tregs for proliferation. The IL-2 KO LHS results show a reduced capacity for Treg proliferation (Fig. 4D). Due to these deficiencies, the IL-2 KO Treg population is never able to expand properly relative to the WT (Fig. 4E). These results suggest that the unique early peripheral Treg population is particularly vulnerable to the lack of IL-2 in these mice.

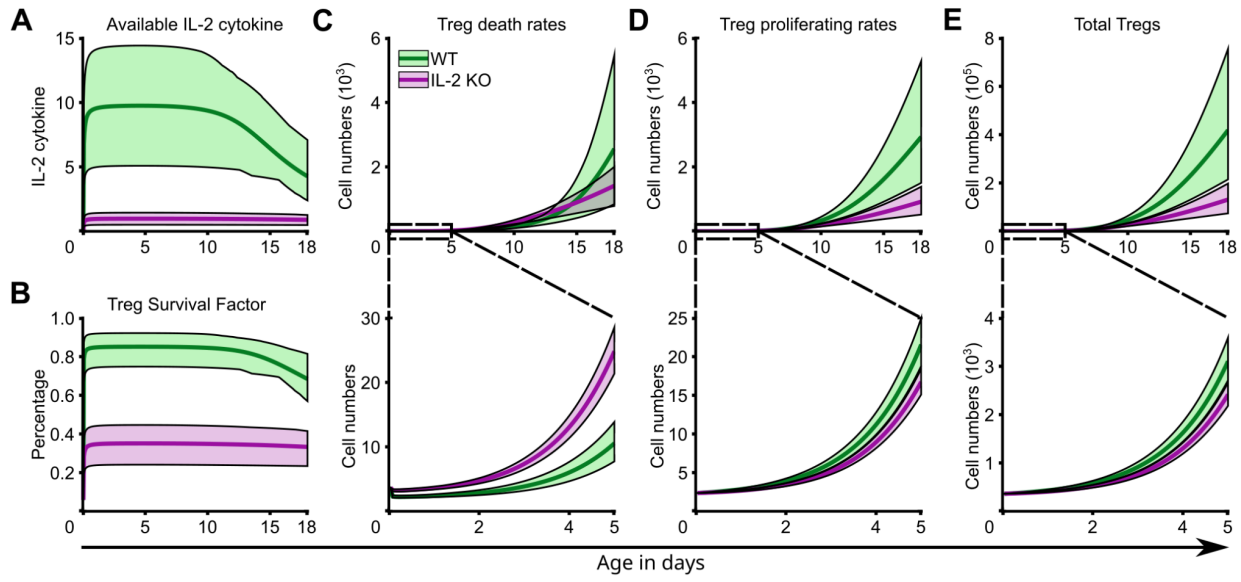

Figure 4 – Impact of IL-2 deficiency on Treg dynamics and survival. The figure presents the results from a range of parameter sampling (+/- 60% LHS sampling range) for parameters γ_R,

$H_{\gamma R}$, p, and p_{KO}, with 3000 simulations conducted. These chosen parameters directly impact Treg's survival. The shaded region represents the range of variability observed across all simulation results, with the top line corresponding to the 90th percentile (representing the upper limit of variability) and the bottom line corresponding to the 10th percentile (representing the lower limit of variability). The solid lines within the shaded region represent the mean values, indicating the average across all simulations. The wild-type data is shown in green, while the IL-2 KO data is shown in pink. (A) The plot illustrates the available IL-2 cytokine in the system, demonstrating its deterministic influence on the (B) Treg Survival Factor. (C-E) Below each plot is a zoomed-in view of the data presented above it. These data represent instantaneous rates of (C) Treg death, (D) Treg proliferation rates, and (E) Total Treg population size.

Parameter Manipulation in IL-2 KO Models: Implications for Treg Functionality and Autoimmune Disease Modulation

Our previous analysis identified deficient expansion trajectories in naive T cells within the IL-2 KO math model compared to the WT counterpart, identifying these as symptomatic markers of the autoimmune state. This decline in naive T cells suggests a potential overstimulation due to inadequate regulatory control. This section investigates and quantifies the differences in suppressive capabilities between WT and autoimmune systems by modifying IL-2 KO model parameters to predict essential suppressive functions for autoimmunity mitigation.

Given the critical role of IL-2 in Treg functionality, its deficiency in the IL-2 KO model reduces Treg-mediated suppression, potentially allowing for unchecked activation of naive T cells. We hypothesize that by manipulating IL-2 KO specific parameters, namely $H_{\beta KO}$ and θ_{KO}, which directly influence Treg suppressive capability, we gain insights into preventing the autoimmune state triggered by the autoimmune activation of naive T cells. These parameters have identical mathematical functions as H_{β} and θ in the WT simulation, but their values are now independent. Through sensitivity analysis (using LHS sampling), we explored parameters H_{β}, θ, $H_{\beta KO}$, and θ_{KO}, aiming to quantify the suppressive difference between genotypes and understand how these differences manifest the autoimmune pathology of the IL-2 KO model. Our objectives were threefold: quantifying the suppressive difference between genotypes, capturing major behavioral differences between WT and IL-2 KO simulations, and analyzing the system's behavior beyond the last point to extrapolate future trends.

By varying these parameters without altering the initial conditions, we observed distinct patterns of increased activation consistent with the autoimmune state in the IL-2 KO simulation (Fig. 5A, top panel). In contrast, the WT simulation exhibited controlled activation after the initial peak. We defined this difference in activation as autoimmune disease in the IL-2 KO simulation. To quantitatively assess the suppressive difference between genotypes, we examined the activation suppressive strength as measured by

$$1 - \left(1 + \left(R\left(\frac{I}{H_I + I}\right)/H_\beta\right)^n\right)$$

(Fig. 5, middle panel) and the rate of activated T cell clearance as measured by

$$\theta RT\left(\frac{I}{H_\theta + I}\right)$$

(Fig. 5, bottom panel). Despite the high variation in parameter values, the Treg suppressive abilities in the WT simulation remained superior and prevented autoimmune disease development.

To evaluate the suppressive deficiencies in the IL-2 KO simulation, we manipulated the initial conditions of IL-2 KO-specific parameters ($H_{\beta KO}$, and θ_{KO}) to determine the necessary adjustments for achieving results similar to the WT system. Increasing the θ_{KO} parameter by 300% resulted in fewer activated T cells than no change (Fig. 5B, top panel). Still, it did not reach the healthy levels of activation seen in the WT simulation. Even with the substantial

variation in parameter values and a three-fold increase in θ_{KO}, we were unable to prevent the autoimmune activation in the IL-2 KO simulation and enhance suppression during critical developmental stages (Fig. 5B middle and bottom panel).

In contrast, reducing the half suppression rate ($H_{\beta KO}$) by 83%, thereby increasing the effectiveness of suppression on naive T cells activation rate (β), brought the autoimmune activation under control in the IL-2 KO simulation, aligning it with the WT (Fig. 5C, top panel). The suppression strength and the rate of activated T cell clearance in the IL-2 KO system surpassed those in the WT during critical developmental stages (Fig. 5C middle and bottom panel), effectively preventing autoimmune disease. As seen in Barron et al. and in our simulation, artificially increasing the survivability of Tregs alone does not rescue the IL-2 KO system from developing autoimmune disease (not shown).

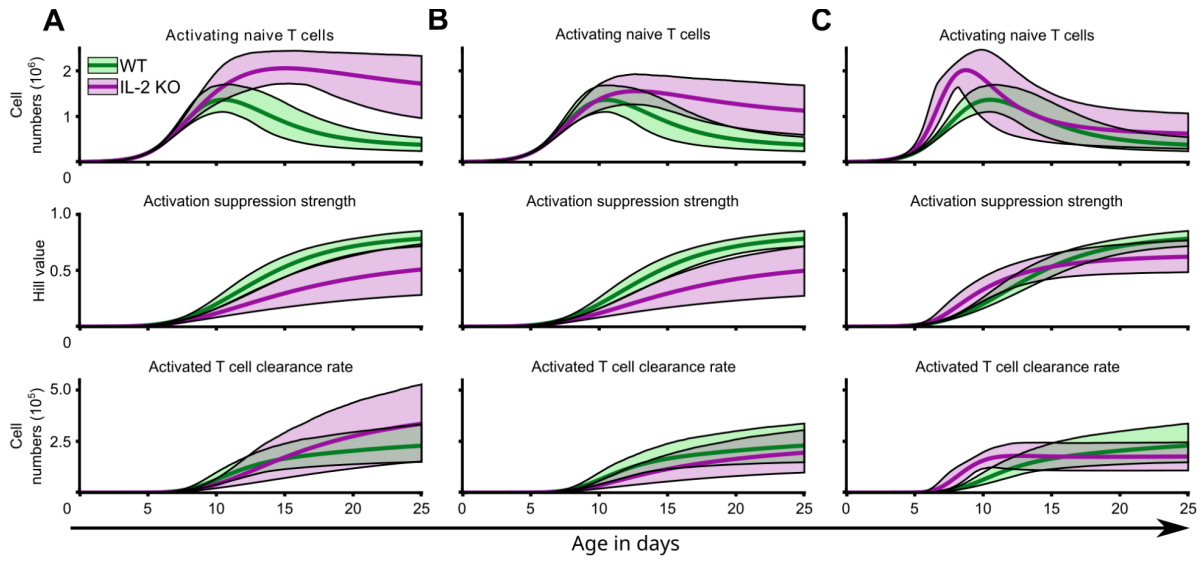

Figure 5 – Parameter-driven prevention of autoimmune activation. The figure showcases the results obtained from a range of parameter sampling (+/- 60% LHS sampling range) for parameters H_{β}, θ, $H_{\beta KO}$, and θ_{KO}, with a total of 3000 simulations conducted. The parameters with the 'KO' subscript have been modified in the IL-2 KO version of the model to explore methodologies for preventing autoimmune disease. Each section has three plots: Top: Activating naive T cells, middle: Activation suppression strength, and bottom: Activated T cell clearance rate. The simulations are analyzed beyond the available data (up to day 18) and extend until day 25. The shaded region represents the range of variability observed across all simulation results, with the top line corresponding to the 90th percentile (representing the upper limit of variability) and the bottom line corresponding to the 10th percentile (representing the lower limit of variability). The solid lines within the shaded region represent the mean values, indicating the average across all simulations. The figure explores different scenarios and parameter modifications to evaluate the prevention of autoimmune disease. Specifically: (A) No change is made to IL-2-specific parameters. (B) The parameter θ_{KO} is increased by 300%. (C) The

half-rate suppression parameter $H_{\beta KO}$ is reduced by 83%, which proportionally increases the suppression of β in the IL-2 KO simulation.

Discussion

The IL-2 cytokine regulates Treg survival and function, preventing autoimmune disease and maintaining immune system balance. Disturbances in IL-2 dynamics, evident in the IL-2 KO mouse model and individuals with systemic lupus erythematosus, can lead to autoimmune disease (16, 59). Because of the IL-2 deficient state of the IL-2 KO mouse model, which invariably develops autoimmune diseases, is valuable for scrutinizing disease development. Nevertheless, autoimmune disease pathogenesis's intricate and multifaceted nature remains ambiguous (15). Using our mathematical model that mirrors the autoimmune condition of the IL-2 KO mouse, we attempt to bridge this knowledge gap by providing a systematic framework to explore the dynamics of autoimmune pathogenesis.

Using experimental data from both WT and IL-2 KO mice, we calibrated our model parameters to closely match the WT and IL-2 KO states, with the latter characterized by increased activation (Fig. 3A Simulation comparison) (17, 18, 60, 61). Calibrating parameters to the data facilitated inference analysis, allowing for a comprehensive comparison of expansion trajectories among identical cellular populations across both genotypes. Relative to the WT simulations, the IL-2

KO displayed deficient expansion trajectories in both naive T cell and Treg populations (Fig. 3B Simulation comparison, Fig. 4, and S.Fig 1). We attribute the observed discrepancies in cellular expansion to symptoms of autoimmunity within our model.

Using Latin Hypercube Sampling, we assessed the impact of Treg death rate parameters on Treg population dynamics, finding that a reduced Treg Survival Factor early in immune development constrains normal proliferation pathways (Fig. 4). In IL-2 KO mice, early peripheral Tregs present before day 3—before robust thymic production begins (62)—are particularly vulnerable to expansion limitations due to IL-2 deficiency. Some of these early Tregs are induced by maternal microchimeric cells (MMc) (48, 63–65), which promote tolerance to non-inherited maternal antigens (NIMA) (66–68) and have been linked to autoimmune diseases (65, 69, 70). Our model indicates that these Tregs likely face restricted expansion in IL-2 deficient environments, but the broader implications of losing this NIMA-tolerant Treg population remain underexplored (71–75).

Tregs exert influence on the homeostatic dynamics of naive T cells, particularly in modulating their activation through interactions with dendritic cells (35–41), and once activated, can also be cleared by Treg cytotoxicity (42–46). We conducted a targeted LHS study to predict which suppressive ability is essential for mitigating autoimmunity. Results of this study show that suppressing the activation rate of naive T cells is critical for preventing autoimmune disease (Fig. 5C). While clearance of activated T cells reduced their numbers, it was insufficient to return activation to similar levels as the WT. Our study indicates that augmenting Treg

suppression via IL-2 supplementation could help mitigate autoimmune diseases (76). Additionally, clinical applications of low-dose IL-2 therapies have demonstrated benefits by bolstering Tregs in individuals with autoimmune disorders or those undergoing graft-versus-host disease treatments (77–81).

While offering valuable insights into IL-2 KO autoimmune activation, our model exhibits limitations that require further refinement. Instead of capturing the steady increase in WT activation, it presents an atypical peak (Fig.3A; column 3, bottom row). This discrepancy, along with differences in naive T cell populations, highlights areas for improvement. Our results show that clearance can limit the number of activated T cells (Fig. 5B); introducing CD8 T cell cytotoxicity may reconcile these discrepancies by facilitating the clearance of excessively activated T cells, aligning simulation results more closely with experimental data (82). A first-order sensitivity analysis shows the renewal rate of naive T cells as the most sensitive parameters (μ, s_n; data not shown). Echoing this, Khailaei et al. found that controlling the renewal rate of naive T cells could modulate the immune system's activation threshold, potentially assisting in distinguishing between self- and non-self-immune responses (31). In these autoimmune models, the system's homeostasis is dependent on fluctuations in the naive T cell population. The next evolution of this model should incorporate the influence of IL-7 cytokine, known for its role in naive T cell homeostasis (83, 84).

Our mathematical model enabled us to simulate the autoimmune state effectively, offering a distinct perspective on the limited expansion potential of early peripheral Tregs and identifying

critical parameter values necessary to prevent the high levels of naive T cell activation seen in the IL-2 KO mice. This work promises fruitful extensions to research involving other autoimmune mouse models, including the CD25 knockout and scurfy mice models (61, 85), with minimal adjustments needed.

References

1. Conrad, N., S. Misra, J. Y. Verbakel, G. Verbeke, G. Molenberghs, P. N. Taylor, J. Mason, N. Sattar, J. J. V. McMurray, I. B. McInnes, K. Khunti, and G. Cambridge. 2023. Incidence, prevalence, and co-occurrence of autoimmune disorders over time and by age, sex, and socioeconomic status: a population-based cohort study of 22 million individuals in the UK. *The Lancet* 401: 1878–1890.
2. Cooper, G. S., M. L. K. Bynum, and E. C. Somers. 2009. Recent insights in the epidemiology of autoimmune diseases: Improved prevalence estimates and understanding of clustering of diseases. *J. Autoimmun.* 33: 197–207.
3. Health, N. I. 2013. *Report of the Director—National Institutes of Health: Fiscal Years 2014–2015*,. National Institutes of Health.
4. Committee, A. D. C. 2005. Progress in autoimmune diseases research. In *Report to Congress. NIH publication* 05–5140.
5. Schmidt, C. W. 2011. Questions persist: Environmental factors in autoimmune disease. .
6. Smyk, D., E. I. Rigopoulou, H. Baum, A. K. Burroughs, D. Vergani, and D. P. Bogdanos. 2012. Autoimmunity and environment: Am I at risk? *Clin. Rev. Allergy Immunol.* 42: 199–212.
7. Rai, E., and E. K. Wakeland. 2011. Genetic predisposition to autoimmunity–what have we learned? *Semin. Immunol.* 23: 67–83.
8. Lee, B., E. W. Holt, R. J. Wong, J. L. Sewell, M. Somsouk, M. Khalili, and M. M. Tana. 2018. Race/ethnicity is an independent risk factor for autoimmune hepatitis among the San Francisco underserved. *Autoimmunity* 51: 258–264.
9. Schiff, M. H., J. M. Kremer, A. Jahreis, E. Vernon, J. D. Isaacs, and R. F. Vollenhoven. 2011. Integrated safety in tocilizumab clinical trials. *Arthritis Res. Ther.* 13: 1–13.
10. Dullemen, H. M., S. J. Deventer, D. W. Hommes, H. A. Bijl, J. Jansen, G. N. Tytgat, and J. Woody. 1995. Treatment of Crohn's disease with anti-tumor necrosis factor chimeric monoclonal antibody (cA2. *Gastroenterology* 109: 129–135.
11. Maini, R., E. W. Clair, F. Breedveld, D. Furst, J. Kalden, M. Weisman, and P. Lipsky. 1999. Infliximab (chimeric anti-tumour necrosis factor α monoclonal antibody) versus placebo in rheumatoid arthritis patients receiving concomitant methotrexate: A randomised phase III trial. *The Lancet* 354: 1932–1939.
12. Group, C. H. S. 1991. A randomized study of the effect of withdrawing hydroxychloroquine sulfate in systemic lupus erythematosus. *N. Engl. J. Med.* 324: 150–154.
13. Dinse, G. E., C. G. Parks, C. R. Weinberg, C. A. Co, J. Wilkerson, D. C. Zeldin, E. K. L. Chan, and F. W. Miller. 2022. Increasing Prevalence of Antinuclear Antibodies in the United States. *Arthritis Rheumatol.* 74: 2032–2041.
14. Miller, F. W. 2023. The increasing prevalence of autoimmunity and autoimmune diseases: an urgent call to action for improved understanding, diagnosis, treatment, and prevention. *Curr. Opin. Immunol.* 80: 102266.
15. Rosenblum, M. D., K. A. Remedios, and A. K. Abbas. 2015. Mechanisms of human autoimmunity. *J. Clin. Invest.* 125: 2228–2233.
16. Hoyer, K. K., H. Dooms, L. Barron, and A. K. Abbas. 2008. Interleukin‐2 in the development and control of inflammatory disease. *Immunol. Rev.* 226: 19–28.
17. Sadlack, B., J. Löhler, H. Schorle, G. Klebb, H. Haber, E. Sickel, and I. Horak. 1995. Generalized autoimmune disease in interleukin‐2‐deficient mice is triggered by an uncontrolled activation and proliferation of CD4+ T cells. *Eur. J. Immunol.* 25: 3053–3059.

18. Valentine, K. M., D. Davini, T. J. Lawrence, G. N. Mullins, M. Manansala, M. Al-Kuhlani, J. M. Pinney, J. K. Davis, A. E. Beaudin, S. S. Sindi, D. M. Gravano, and K. K. Hoyer. 2018. CD8 Follicular T Cells Promote B Cell Antibody Class Switch in Autoimmune Disease. *J. Immunol.* 201: 31–40.
19. Gravano, D. M., M. Al-Kuhlani, D. Davini, P. D. Sanders, J. O. Manilay, and K. K. Hoyer. 2016. CD8+ T cells drive autoimmune hematopoietic stem cell dysfunction and bone marrow failure. *J. Autoimmun.* 75: 58–67.
20. Zhu, J., X. Liu, C. Xie, M. Yan, Y. Yu, E. S. Sobel, E. K. Wakeland, and C. Mohan. 2005. T cell hyperactivity in lupus as a consequence of hyperstimulatory antigen-presenting cells. *J. Clin. Invest.* 115: 1869–1878.
21. Han, B. K., A. M. White, K. H. Dao, D. R. Karp, E. K. Wakeland, and L. S. Davis. 2005. Increased prevalence of activated CD70+CD4+ T cells in the periphery of patients with systemic lupus erythematosus. *Lupus* 14: 598–606.
22. Naganuma, M., M. Watanabe, T. Kanai, Y. Iwao, M. Mukai, H. Ishii, and T. Hibi. 2002. Characterization of structures with T-lymphocyte aggregates in ileal villi of Crohn's disease. *Am. J. Gastroenterol.* 97: 1741–1747.
23. Blumberg, R. S., and W. Strober. 2001. Prospects for Research in Inflammatory Bowel Disease. *JAMA* 285: 643–647.
24. Eastaff-Leung, N., N. Mabarrack, A. Barbour, A. Cummins, and S. Barry. 2010. Foxp3+ Regulatory T Cells, Th17 Effector Cells, and Cytokine Environment in Inflammatory Bowel Disease. *J. Clin. Immunol.* 30: 80–89.
25. Mudter, J., and M. F. Neurath. 2003. Mucosal T cells: mediators or guardians of inflammatory bowel disease? *Curr. Opin. Gastroenterol.* 19: 343–349.
26. Toh, M.-L., and P. Miossec. 2007. The role of T cells in rheumatoid arthritis: new subsets and new targets. *Curr. Opin. Rheumatol.* 19: 284–288.
27. Dattner, I., H. Ship, and E. O. Voit. 2020. Separable Nonlinear Least-Squares Parameter Estimation for Complex Dynamic Systems. *Complexity* 2020: e6403641.
28. Shampine, L. F., and M. W. Reichelt. 1997. The MATLAB ODE Suite. *SIAM J. Sci. Comput.* 18: 1–22.
29. Shampine, L. F., M. W. Reichelt, and J. A. Kierzenka. 1999. Solving Index-1 DAEs in MATLAB and Simulink. *SIAM Rev.* 41: 538–552.
30. Blok, R. 2022. lhsdesigncon (https://github.com/rikblok/matlab-lhsdesigncon), GitHub. Retrieved September 9, 2022. .
31. Khailaie, S., F. Bahrami, M. Janahmadi, P. Milanez-Almeida, J. Huehn, and M. Meyer-Hermann. 2013. A mathematical model of immune activation with a unified self-nonself concept. *Front. Immunol.* 4: 474.
32. Setoguchi, R., S. Hori, T. Takahashi, and S. Sakaguchi. 2005. Homeostatic maintenance of natural Foxp3+ CD25+ CD4+ regulatory T cells by interleukin (IL)-2 and induction of autoimmune disease by IL-2 neutralization. *J. Exp. Med.* 201: 723–735.
33. Boyman, O., and J. Sprent. 2012. The role of interleukin-2 during homeostasis and activation of the immune system. *Nat. Rev. Immunol.* 12: 180–190.
34. Malek, T. R. 2008. The Biology of Interleukin-2. *Annu. Rev. Immunol.* 26: 453–479.
35. Tang, Q. 2006. Visualizing regulatory T cell control of autoimmune responses in nonobese diabetic mice. *Nat. Immunol* 7: 83–92.
36. Tadokoro, C. E. 2006. Regulatory T cells inhibit stable contacts between CD4+ T cells and dendritic cells in vivo. *J Exp Med* 203: 505–511.

37. Misra, N., J. Bayry, S. Lacroix-Desmazes, M. D. Kazatchkine, and S. V. Kaveri. 2004. Cutting edge: Human CD4+ CD25+ T cells restrain the maturation and antigen-presenting function of dendritic cells. *J Immunol* 172: 4676–4680.
38. Houot, R., I. Perrot, E. Garcia, and S. Durand ILebecque. 2006. Human CD4+ CD25 high regulatory T cells modulate myeloid but not plasmacytoid dendritic cells activation. *J Immunol* 176: 5293–5298.
39. Veldhoen, M., H. Moncrieffe, R. J. Hocking, C. J. Atkins, and B. Stockinger. 2006. Modulation of dendritic cell function by naive and regulatory CD4 + T cells. *J Immunol* 176: 6202–6210.
40. Lewkowich, I. P., N. S. Herman, K. W. Schleifer, M. P. Dance, B. L. Chen, and K. M. Dienger. 2005. CD4+ CD25+ T cells protect against experimentally induced asthma and alter pulmonary dendritic cell phenotype and function. *J Exp Med* 202: 1549–1561.
41. Serra, P., A. Amrani, J. Yamanouchi, B. Han, S. Thiessen, and T. Utsugi. 2003. CD40 ligation releases immature dendritic cells from the control of regulatory CD4+ CD25+ T cells. *Immunity* 19: 877–889.
42. Grossman, W. J. 2004. Differential expression of granzymes A and B in human cytotoxic lymphocyte subsets and T regulatory cells. *Blood* 104: 2840–2848.
43. McHugh, R. S. 2002. CD4+ CD25+ immunoregulatory T cells: Gene expression analysis reveals a functional role for the glucocorticoid-induced TNF receptor. *Immunity* 16: 311–323.
44. Gondek, D. C., L. F. Lu, S. A. Quezada, S. Sakaguchi, and R. J. Noelle. 2005. Cutting edge: Contact-mediated suppression by CD4+ CD25+ regulatory cells involves a granzyme B-dependent, perforin-independent mechanism. *J Immunol* 174: 1783–1786.
45. Lindqvist, C. A., L. H. Christiansson, I. Thörn, S. Mangsbo, G. Paul-Wetterberg, C. Sundström, T. H. Tötterman, B. Simonsson, G. Enblad, P. Frisk, U. Olsson-Strömberg, and A. S. I. Loskog. 2011. Both CD4+ FoxP3+ and CD4+ FoxP3− T cells from patients with B-cell malignancy express cytolytic markers and kill autologous leukaemic B cells in vitro. *Immunology* 133: 296–306.
46. Cao, X., S. F. Cai, T. A. Fehniger, J. Song, L. I. Collins, D. R. Piwnica-Worms, and T. J. Ley. 2007. Granzyme B and Perforin Are Important for Regulatory T Cell-Mediated Suppression of Tumor Clearance. *Immunity* 27: 635–646.
47. Ermann, J., V. Szanya, G. S. Ford, V. Paragas, C. G. Fathman, and K. Lejon. 2001. CD4+CD25+ T Cells Facilitate the Induction of T Cell Anergy. *J. Immunol.* 167: 4271–4275.
48. Wrenshall, L. E., E. T. Stevens, D. R. Smith, and J. D. Miller. 2007. Maternal microchimerism leads to the presence of interleukin-2 in interleukin-2 knock out mice: Implications for the role of interleukin-2 in thymic function. *Cell. Immunol.* 245: 80–90.
49. Katzman, S. D., K. K. Hoyer, H. Dooms, I. K. Gratz, M. D. Rosenblum, J. S. Paw, S. H. Isakson, and A. K. Abbas. 2011. Opposing functions of IL-2 and IL-7 in the regulation of immune responses. *Cytokine* 56: 116–121.
50. Chaudhry, A. 2011. Interleukin-10 signaling in regulatory T cells is required for suppression of Th17 cell-mediated inflammation. *Immunity* 34: 566–578.
51. Xia, J. 2010. IL-15 promotes regulatory T cell function and protects against diabetes development in NK-depleted NOD mice. *Clin. Immunol.* 134: 130–139.
52. Milanez‐Almeida, P., M. Meyer‐Hermann, A. Toker, S. Khailaie, and J. Huehn. 2015. Foxp3+ regulatory T‐cell homeostasis quantitatively differs in murine peripheral lymph nodes and spleen. *Eur. J. Immunol.* 45: 153–166.
53. Suffner, J., K. Hochweller, M. C. Kühnle, X. Li, R. A. Kroczek, N. Garbi, and G. J.

Hämmerling. 2010. Dendritic cells support homeostatic expansion of Foxp3+ regulatory T cells in Foxp3. LuciDTR mice. *J. Immunol.* 184: 1810–1820.
54. Bensinger, S. J., P. T. Walsh, J. Zhang, M. Carroll, R. Parsons, J. C. Rathmell, C. B. Thompson, M. A. Burchill, M. A. Farrar, and L. A. Turka. 2004. Distinct IL-2 Receptor Signaling Pattern in CD4+CD25+ Regulatory T Cells1. *J. Immunol.* 172: 5287–5296.
55. Kovanen, P. E., L. Young, A. Al-Shami, V. Rovella, C. A. Pise-Masison, M. F. Radonovich, J. Powell, J. Fu, J. N. Brady, P. J. Munson, and W. J. Leonard. 2005. Global analysis of IL-2 target genes: identification of chromosomal clusters of expressed genes. *Int. Immunol.* 17: 1009–1021.
56. Bayer, A. L., A. Yu, D. Adeegbe, and T. R. Malek. 2005. Essential role for interleukin-2 for CD4+CD25+ T regulatory cell development during the neonatal period. *J. Exp. Med.* 201: 769–777.
57. Chougnet, C. A., P. Tripathi, C. S. Lages, J. Raynor, A. Sholl, P. Fink, D. R. Plas, and D. A. Hildeman. 2011. A Major Role for Bim in Regulatory T Cell Homeostasis. *J. Immunol.* 186: 156–163.
58. Barron, L., H. Dooms, K. K. Hoyer, W. Kuswanto, J. Hofmann, W. E. O'Gorman, and A. K. Abbas. 2010. Cutting edge: Mechanisms of IL-2–dependent maintenance of functional regulatory T cells. *J. Immunol.* 185: 6426–6430.
59. Lieberman, L. A., and G. C. Tsokos. 2010. The IL-2 defect in systemic lupus erythematosus disease has an expansive effect on host immunity. *J. Biomed. Biotechnol.* 2010: 740619.
60. Hoyer, K. K., W. F. Kuswanto, E. Gallo, and A. K. Abbas. 2009. Distinct roles of helper T-cell subsets in a systemic autoimmune disease. *Blood* 113: 389–395.
61. Mullins, G. N., K. M. Valentine, M. Al-Kuhlani, D. Davini, K. D. C. Jensen, and K. K. Hoyer. 2020. T cell signaling and Treg dysfunction correlate to disease kinetics in IL-2Rα-KO autoimmune mice. *Sci. Rep.* 10: 21994.
62. Asano, M., M. Toda, N. Sakaguchi, and S. Sakaguchi. 1996. Autoimmune disease as a consequence of developmental abnormality of a T cell subpopulation. *J. Exp. Med.* 184: 387–396.
63. Mold, J. E., J. Michaëlsson, T. D. Burt, M. O. Muench, K. P. Beckerman, M. P. Busch, T.-H. Lee, D. F. Nixon, and J. M. McCune. 2008. Maternal Alloantigens Promote the Development of Tolerogenic Fetal Regulatory T Cells in Utero. *Science* 322: 1562–1565.
64. Michaëlsson, J., J. E. Mold, J. M. McCune, and D. F. Nixon. 2006. Regulation of T Cell Responses in the Developing Human Fetus1. *J. Immunol.* 176: 5741–5748.
65. Adams, K. M., and J. L. Nelson. 2004. MicrochimerismAn Investigative Frontier in Autoimmunity and Transplantation. *JAMA* 291: 1127–1131.
66. Molitor-Dart, M. L., J. Andrassy, J. Kwun, H. A. Kayaoglu, D. A. Roenneburg, L. D. Haynes, J. R. Torrealba, J. L. Bobadilla, H. W. Sollinger, S. J. Knechtle, and W. J. Burlingham. 2007. Developmental Exposure to Noninherited Maternal Antigens Induces CD4+ T Regulatory Cells: Relevance to Mechanism of Heart Allograft Tolerance1. *J. Immunol.* 179: 6749–6761.
67. Akiyama, Y., S. M. Caucheteux, C. Vernochet, Y. Iwamoto, K. Tanaka, C. Kanellopoulos-Langevin, and G. Benichou. 2011. Transplantation Tolerance to a Single Noninherited MHC Class I Maternal Alloantigen Studied in a TCR-Transgenic Mouse Model. *J. Immunol.* 186: 1442–1449.
68. Matsuoka, K., T. Ichinohe, D. Hashimoto, S. Asakura, M. Tanimoto, and T. Teshima. 2006. Fetal tolerance to maternal antigens improves the outcome of allogeneic bone marrow transplantation by a CD4+CD25+ T-cell–dependent mechanism. *Blood* 107: 404–409.

69. vanZyl, B., R. Planas, Y. Ye, A. Foulis, R. R. deKrijger, M. Vives-Pi, and K. M. Gillespie. 2010. Why are levels of maternal microchimerism higher in type 1 diabetes pancreas? *Chimerism* 1: 45–50.
70. Roy, E., M. Leduc, S. Guegan, L. Rachdi, N. Kluger, R. Scharfmann, S. Aractingi, and K. Khosrotehrani. 2011. Specific maternal microchimeric T cells targeting fetal antigens in β cells predispose to auto-immune diabetes in the child. *J. Autoimmun.* 36: 253–262.
71. Leveque, L., and K. Khosrotehrani. 2011. Can maternal microchimeric cells influence the fetal response toward self antigens? *Chimerism* 2: 71–77.
72. Leveque, L., and K. Khosrotehrani. 2014. Feto-maternal allo-immunity, regulatory T cells and predisposition to auto-immunity. *Chimerism* .
73. Artlett, C. M., F. W. Miller, L. G. Rider, and for the Childhood Myositis Heterogeneity Collaborative Study Group. 2001. Persistent maternally derived peripheral microchimerism is associated with the juvenile idiopathic inflammatory myopathies. *Rheumatology* 40: 1279–1284.
74. Khosrotehrani, K., S. Guegan, S. Fraitag, M. Oster, Y. de Prost, C. Bodemer, and S. Aractingi. 2006. Presence of Chimeric Maternally Derived Keratinocytes in Cutaneous Inflammatory Diseases of Children: The Example of Pityriasis Lichenoides. *J. Invest. Dermatol.* 126: 345–348.
75. Lambert, N. C., T. D. Erickson, Z. Yan, J. M. Pang, K. A. Guthrie, D. E. Furst, and J. L. Nelson. 2004. Quantification of maternal microchimerism by HLA-specific real-time polymerase chain reaction: Studies of healthy women and women with scleroderma. *Arthritis Rheum.* 50: 906–914.
76. Grinberg-Bleyer, Y. 2010. IL-2 reverses established type 1 diabetes in NOD mice by a local effect on pancreatic regulatory T cells. *J. Exp. Med.* 207: 1871–1878.
77. Koreth, J. 2011. Interleukin-2 and regulatory T cells in graft-versus-host disease. *N Engl J* 365: 2055–2066.
78. Long, S. A. 2012. Diabetes TrialNet and the Immune Tolerance Network. .
79. Saadoun, D. 2011. Regulatory T-cell responses to low-dose interleukin-2 in HCV-induced vasculitis.N Engl J Med365:2067–2077.15. .
80. He, J. 2016. *Low-dose interleukin-2 treatment selectively modulates CD4(+)T cell subsets in patients with systemic lupus erythematosus.Nat*,. 991–993, Med22.
81. Whitehouse, G., E. Gray, S. Mastoridis, E. Merritt, E. Kodela, J. H. M. Yang, R. Danger, M. Mairal, S. Christakoudi, and J. J. Lozano. 2017. IL-2 therapy restores regulatory T-cell dysfunction induced by calcineurin inhibitors. *Proc Natl Acad Sci USA* 114: 7083–7088.
82. Gravano, D. M., and K. K. Hoyer. 2013. Promotion and prevention of autoimmune disease by CD8+ T cells. *J. Autoimmun.* 45: 68–79.
83. Schluns, K. S., W. C. Kieper, S. C. Jameson, and L. Lefrançois. 2000. Interleukin-7 mediates the homeostasis of naïve and memory CD8 T cells in vivo. *Nat. Immunol.* 1: 426–432.
84. Capitini, C. M., A. A. Chisti, and C. L. Mackall. 2009. Modulating T-cell homeostasis with IL-7: preclinical and clinical studies. *J. Intern. Med.* 266: 141–153.
85. Brunkow, M. E., E. W. Jeffery, K. A. Hjerrild, B. Paeper, L. B. Clark, S. A. Yasayko, and F. Ramsdell. 2001. Disruption of a new forkhead/winged-helix protein, scurfin, results in the fatal lymphoproliferative disorder of the scurfy mouse. *Nat. Genet.* 27: 68–73.